Available online at www.sciencedirect.com
SCIENCE DIRECT®
Journal of Computational Physics 203 (2005) 650–667
JOURNAL OF COMPUTATIONAL PHYSICS
www.elsevier.com/locate/jcp

Propagator methods for plasma simulations: application to breakdown

C. Wichaidit *, W.N.G. Hitchon

Department of Electrical and Computer Engineering, University of Wisconsin, Madison, WI 53706, USA

Received 26 January 2004; received in revised form 22 September 2004; accepted 22 September 2004
Available online 22 October 2004

Abstract

Accurate simulation of plasmas often requires a solution of the kinetic equation, either directly by solving the Boltzmann equation (BE) or indirectly by means of 'particle' simulations. However, kinetic simulations are still too computationally intensive for many large scale 3D simulations. In this paper we examine the matching between a kinetic simulation and fluid models which we use in conjunction to form a 'hybrid' plasma model of the breakdown process. The kinetic model is tested for convergence with respect to mesh size Δx and time-step Δt. We then implement fluid models in an attempt to reproduce the results of the kinetic model. To do this it is necessary to have a fluid model which provides accurate simulations with a wide range of Δx and Δt. We accomplish this by means of a propagator (or Green's function) approach. The propagator method reduces to a finite difference scheme at small $\Delta x, \Delta t$ and gives correct results across a wide range of parameters. For intermediate $\Delta x, \Delta t$ it is necessary to take considerable care to derive the correct propagator. We apply the propagator method to two fluid models; one uses parameters which are functions of the electric field, and the other one uses parameters which are functions of the mean kinetic energy (this version also explicitly conserves energy locally). The details of the fluid models employed make a profound difference to the prediction of the breakdown.

Keywords: Plasma simulation; Kinetic model; Convective scheme; Propagator method; Fluid model; Energy-conserving scheme

1. Introduction

The purpose of this paper is to examine the effectiveness of numerical techniques for the simulation of electrical breakdown of a gas. Breakdown is in some regards more difficult to simulate than other aspects of plasma behavior. During the initial phases of breakdown the electron density is expected to grow exponentially in time (and sometimes in space). Modest differences in the predicted ionization rate [1,2] can lead to

* Corresponding author.
E-mail addresses: wichaidi@cae.wisc.edu (C. Wichaidit), hitchon@engr.wisc.edu (W.N.G. Hitchon).

0021-9991/$ - see front matter © 2004 Elsevier Inc. All rights reserved.
doi:10.1016/j.jcp.2004.09.008

very large differences in density in this phase. Alternatively, near the threshold for the onset of breakdown there is a sensitive region where we may predict growth or decay in the density, and only small changes in parameters or models are needed to make the difference between one or the other.

The most accurate simulation of breakdown calls for a kinetic treatment, such as the solution of the Boltzmann equation (BE) for the charged particle distribution function, or the numerical simulation of motions of charged particles. There are numerous plasma simulations using kinetic treatments such as [3–8]. However, kinetic simulation describes the plasma in great detail and is very computationally intensive in practical situations so it is desirable to have a fluid equation for the charged particle density which approximates the behavior predicted by the BE. Fluid simulations have been abundantly described; [17–21]. Such simulation is frequently attempted using a variety of 'hybrid' codes [9]. In a hybrid code, detailed calculations at the level of the BE are done to calibrate a fluid calculation (providing values for quantities such as the diffusion coefficient D, the mobility μ, the ionization rate S, and so on).

A key parameter in the fluid model employed here is the fraction, α, of the energy which is put into ionization, as opposed to excitation or other inelastic processes (or radiation losses). In effect, the solution of the BE provides the local value of α, as a function of the other variables. α can vary significantly, and this variation is largely what provides the range of possible final densities.

Any model which conserves energy, even approximately, and which uses the correct α (which may mean using an approach in which α is never explicitly employed, but which nevertheless results in the right fraction of the energy being put into ionization) will give roughly the right amount of electrons. This is especially true in a homogeneous plasma. Inert gases (Xe, Ne, Ar, etc.) should have a very high α which makes modeling them more straightforward.

We have examined the capability of fluid models to reproduce the behavior of the BE, in order to assess how accurate a fluid model of breakdown can be made. One issue of some concern was the value of the Δx and the Δt which can be used. The BE solution requires very small values of Δx and Δt, because the natural scales of the problem are rather short. It is of some concern whether the fluid equation must be restricted to the same range of Δx and Δt. We thus employed a 'propagator' (Green's function) method [38–41] to solve the fluid equations (similar to our BE solution technique) which works well for a wide range of Δx and Δt.

The propagator method is of some interest in itself. It provides a simple scheme for solving a discretized fluid equation, which can be reduced to a finite difference scheme for small $\Delta x, \Delta t$ but which works equally well for a wide range of $\Delta x, \Delta t$ since the propagator does not necessarily obey the Courant limit. One version of the scheme has been implemented in a form which explicitly and locally conserves particles and energy. The finite difference forms of the fluid equations involve evaluating derivatives; in this problem those derivatives are not necessarily well described by finite differences because the gradients are very steep indeed. The propagator does not require the calculation of derivatives and is easier to implement than the finite difference scheme.

Eastwood [39,40] has presented a rather general treatment of methods of characteristics, including Lagrangian schemes, applied to a one dimensional fluid flow. Eastwood distinguished a number of different ways of handling the problem, and although our methods do not entirely fall within his framework, there are some aspects of his categorization which are illuminating. The most pertinent distinction between schemes, from our point of view, reflects whether the scheme (a) takes an initial density defined on mesh points and propagates it forward in time, along the characteristics, or (b) if the scheme focuses on a final cell and looks back along the trajectory to find the initial density. In case (b), when looking back along the trajectory one is (in general) forced to interpolate between mesh points to find the 'old' density on the trajectory/characteristic. Case (a) requires that density from an 'old' mesh point be propagated forward and then shared between mesh points. Eastwood prefers case (b) for reasons of accuracy in the problem he was studying. We find compelling reasons to use case (a) which we shall point out shortly. The review paper by Staniforth and Cote [44] considers Eastwood's work, but their discussion is limited to case (b), as their Figs. 1 and 2 show. These figures define what we mean by 'looking back along a trajectory' very clearly. The

density at a mesh point labeled C at time $t_n + \Delta t$ is equal to the density at time $t_n - \Delta t$, at a point A which does not lie on the mesh. The problem, for them, is in large part to locate the point A and to interpolate to find the density at point A. As they remark in their conclusions, the class of schemes they consider does not in general formally conserve quantities (but they do appear to behave acceptably). This last point is a critical one, for us. We discovered very soon [45] that for simulations of electron systems, it was imperative to conserve numbers and energy (and sometimes other quantities such as angular momentum) very precisely. A scheme which falls in case (a) can be made to do this, by focusing on conservation as applied to the contents of one initial cell at a time. We have remarked on this in a number of publications. Such careful conservation, particularly of energy, was not the main concern for Eastwood. Case (a) is distinct from other Lagrangian/method of characteristics approaches, in this important regard, which allows us to build in conservation laws. A similar approach was taken more recently by Leslie and Purser [46,47], who also note the possibility of achieving mass conservation, and by others who have built on their work (such as [48]). They construct 'forward trajectories' and employ cascade interpolation, which consists of a series of 1D interpolations. Conservation is not automatic, but can be achieved. Their interpolation is thus not equivalent to ours (the propagator method). Conservation seems to be more straightforward in our scheme. Most importantly for the present paper, one of the issues which we address here concerns how to build diffusion into the propagator while maintaining the correct drift velocity. Staniforth and Cote do not include diffusion in their treatment; this simplifies the problem greatly. In our case the accuracy of the scheme in the presence of diffusion is critical, and this is the main point which we address here.

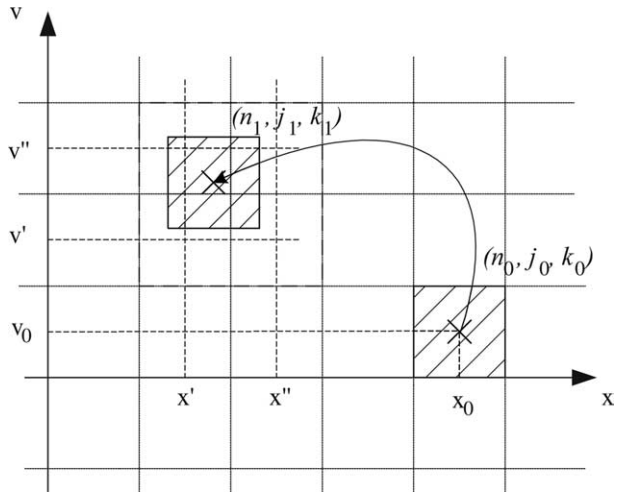

Fig. 1. Schematic of the moving cell launched from (n_0, j_0, k_0) and moving to its final position centered at (n_1, j_1, k_1). Particles are then put back into mesh cells.

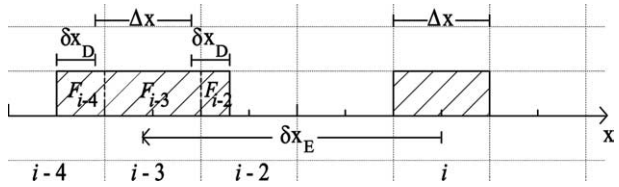

Fig. 2. A simple propagator for the particles initially in the mesh cell i moves (for example) a distance $\delta x_E = -3.1\Delta x$ and expands both sides by $\delta x_D = 0.4\Delta x$ after a time-step Δt. Fractions F_{i-4}, F_{i-3}, and F_{i-2} of the propagator overlap the mesh cells $i-4$, $i-3$, and $i-2$, respectively.

2. Numerical models

Several numerical models have been employed and developed to characterize the breakdown of a gas. In this paper, we first employ a kinetic model, the convective scheme or CS (which was described earlier in [9,10]) to describe the electron distribution function (EDF) during the breakdown phase. The CS will be briefly described next. Second, a fluid model based on a 'propagator' method is developed. To get good agreement with the kinetic model, the values of transport parameters and some reaction rates from the CS are used in the 'propagator' model. The proposed 'propagator' model will be described and validated in Section 2.2. Later in Section 3, the results from kinetic and fluid simulations will be discussed and compared, and simulations using the the kinetic and fluid models in an AC field will also be performed.

2.1. Kinetic model – convective scheme

In this section we briefly recap the main features of the BE solver, which we refer to as the CS. The CS has been applied to a wide range of transport problems in plasma applications and discussed in [11–16]. The CS uses a distribution function defined as a density in a cell while particle methods such as particle-in-cell and Monte Carlo use super particles. Given a fixed mesh which consists of the cells into which phase space is divided, moving cells move particles by stepping in time to the final positions, x, associated with the components of the velocity parallel and perpendicular to the x axis, $(v_x, v_\perp)$, together with the applied field. The mesh cell is assigned values of (1) position x, (2) speed, v and (3) the direction cosine of the velocity relative to the x axis, μ, which can be discretized using labels (n,j,k). In Fig. 1, the initial cell centered at (n_0,j_0,k_0) moves to a new position with its center in the cell labeled by (n_1,j_1,k_1) according to the equations of motion [10]

$$\Delta x = \boldsymbol{v}\Delta t, \tag{1}$$

$$\Delta \boldsymbol{v} = \frac{q}{m_e}\boldsymbol{E}\Delta t, \tag{2}$$

and then its contents are carefully put back into the neighboring mesh cells corresponding to positions x', x'', speed v', v'', and directions μ', μ'' (not shown). The numbers put back in each cell are determined by an 'overlap rule' [9,10]; the number of particles is exactly conserved. This scheme also conserves the total energy of the particles by considering the total energy of the particles in the initial cell, and the potential energy in each spatial cell into which the particles are being put back. By taking the potential energy to be constant within each spatial mesh cell, the new kinetic energy of particles that are added back into each spatial cell considered separately can be calculated from the initial total energy and the potential energy of the final cell (which in general is different at x' and x''). In other words, the kinetic energy of particles put back at x' is different from that for particles put back at x'', but the average total energy is the same in both cells, since they are both equal to the initial total energy of a single particle. (When many cells are taken together, the fate of them all shows how the phase space volume evolves, much as the many particles in a particle simulation do, since the motion of a CS cell reflects the motions of the particles within it.)

The CS model was tested for convergence with respect to Δx, and Δt. It was found, as usual, that $\Delta x \lesssim \lambda_{el}/2$, $\Delta t \lesssim 0.1\tau_c$ (where λ_{el} is elastic mean free path, and τ_c is the elastic collision time) were necessary.

2.2. Propagator method – fluid model

The objective in this paper is to examine the accuracy of various approaches to describing the breakdown of a gas. In addition to the kinetic model, one of the tools we need is a fluid model of a plasma.

Many techniques have been developed to solve transport (fluid) equations such as ones reported by Wu et al. [30] and Elta et al. [31]. In this paper we propose a fluid model which works well for arbitrary sizes of Δx and Δt. For each particle species the single-particle density (which is space and time dependent) can be written as

$$f(x,t) = \int\int \mathscr{P}(x,t;x',t')f(x',t')\mathrm{d}x', \quad t > t', \tag{3}$$

where the kernel of the integral, $\mathscr{P}(x, t; x', t')$, is the propagator for a particle at position x' at time t'. A simple version and discussion of this propagator were given earlier by Adams et al. [41]. The propagator in principle updates the position of an initial delta function density. In this paper we develop a propagator for an initial density which is unity in a short region of length Δx, and zero elsewhere, i.e. in a cell of a mesh, since this is the appropriate equivalent to the delta function in numerical calculations. This fluid model consists of a simple propagator method which is able to describe the final position of the contents of a moving cell after a time step Δt. This 'propagator' is approximated by moving the initial cell a distance δx_{E}, to describe the effect of the applied electric field $\boldsymbol{E}$, where

$$\delta x_{\mathrm{E}} = \mu_{\mathrm{eff}}\boldsymbol{E}\Delta t, \tag{4}$$

and allowing both of its ends to expand outwards by an additional distance δx_{D} to describe diffusion

$$\delta x_{\mathrm{D}} = \begin{cases} D_{\mathrm{eff}}(\Delta t/\Delta x) & \text{if } \Delta t \text{ is small,} \\ \sqrt{2D_{\mathrm{eff}}\Delta t} & \text{if } \Delta t \text{ is large.} \end{cases} \tag{5}$$

μ_{eff} and D_{eff} denote the effective mobility and effective diffusion coefficient respectively which will be described more in Section 2.2.4. We combine these forms of δx_{D} by adding them reciprocally. In the cases we examine below, Δt is small enough so that the small Δt form of δx_{D} is always used.

A simple overlap rule [9] (illustrated by example in Fig. 2) then implies that the fractions F_j going to the neighboring cell j in time Δt are given by

$$F_j = \frac{\delta x_j}{C_l}, \tag{6}$$

where δx_j is the length of the portion of the moving cell which overlaps final cell j. $C_l = \Delta x + 2\delta x_{\mathrm{D}}$ is the full length of the moving cell.

In the schematic of the propagator shown in Fig. 2, we can find the mean displacement $\delta\bar{x}$ from

$$\delta\bar{x} = F_{i-4}(-4\Delta x) + F_{i-3}(-3\Delta x) + F_{i-2}(-2\Delta x), \tag{7}$$

where

$$F_{i-4} = \frac{|\,\delta x_{\mathrm{E}}\,| + \delta x_{\mathrm{D}} - 3\Delta x}{\Delta x + 2\delta x_{\mathrm{D}}}, \tag{8}$$

$$F_{i-3} = \frac{\Delta x}{\Delta x + 2\delta x_{\mathrm{D}}}, \tag{9}$$

$$F_{i-2} = \frac{\delta x_{\mathrm{D}} - |\,\delta x_{\mathrm{E}}\,| + 3\Delta x}{\Delta x + 2\delta x_{\mathrm{D}}}. \tag{10}$$

Eqs. (7)–(10) yield $\delta\bar{x} \approx -3.1\Delta x = \delta x_{\mathrm{E}}$ but the agreement is not exact. Unfortunately, it turns out that this propagator usually does not give the correct $\delta\bar{x} = \delta x_{\mathrm{E}}$ when δx_{E}, $\delta x_{\mathrm{D}} < \Delta x$; it is necessary to apply a correction to δx_{E} which will be discussed next.

2.2.1. Mean displacement correction

The propagator model works well for values of $\delta x_E, \delta x_D \gg \Delta x$ and gives exactly the right mean displacement $\delta\bar{x} = \delta x_E$ when $\delta x_D = 0$. (If $\delta x_D = 0$, only two values of F (F_{i-4} and F_{i-3} in the example above) are needed, so Eq. (10) for F_{i-2} does not apply.) However, for $\delta x_E, \delta x_D \lesssim \Delta x$ (for both $\delta x_E > \delta x_D$ and $\delta x_D > \delta x_E$ cases), finite mesh size effects mean that using a straightforward overlap rule to map the moving cell back to the mesh yields $\delta\bar{x} \neq \delta x_E$. An example of this is shown in Fig. 3. From Fig. 3, the mean displacement would be

$$\delta\bar{x} = \frac{|\,\delta x_E\,| + \delta x_D}{\Delta x + 2\delta x_D}(-\Delta x). \tag{11}$$

Substituting values of δx_E and δx_D into (11) yields $\delta\bar{x} = -0.36\Delta x$ which is not equal to δx_E. To get the correct mean displacement, a correction for δx_E, $\delta x'_E$ must be used, where in this one case

$$\delta x'_E = -\left[\frac{|\,\delta x_E\,|}{\Delta x}(\Delta x + 2\delta x_D) - \delta x_D\right]. \tag{12}$$

Then substituting (12) instead of δx_E in (11) gives the correct mean distance, $\delta\bar{x} = \delta x_E$.

All the different cases are discussed in Appendix A, where the values of $\delta x'_E$ which result in $\delta\bar{x} = \delta x_E$ (as in Eq. (4)) are given. The corrections are for the case $\delta x_E < 0$.

2.2.2. Conservation of energy

The present method of conservation of energy explicitly employs the potential energy in each cell to find the kinetic energy. Particles which fall from one cell to the next pick up exactly the potential energy difference between the cells. Suppose a group of electrons initially has mean energy of κ (see Fig. 4(a)). The cell (of length Δx) they are in will move by δx_E and expand in length by δx_D at both ends according to Eqs. 4 and 5 (shown in Fig. 4). Finally, some fraction of electrons in the group (determined by the cell length of the moving cell and the overlap length between the moving cell and the fixed cell) gains potential energy of ΔW ($=q\Delta V$) and is put in the final cell where they have the final mean energy of $\kappa + \Delta W$. The rest of the group stay in the initial cell with the same energy they originally had as shown in Fig. 4(c). A carefully set up FD scheme does reproduce this, as we shall see below, but it may be more complicated to ensure energy conservation. The effect of using various schemes to handle the calculation of the rates is shown in the next section. [1]

[1] As an aside, we note that there are circumstances in which it would be appropriate to allow particles which have moved upstream to be said to have the same average energy as the group of particles they started in. In equilibrium the distribution is expected to be a Maxwellian with the same temperature (but different density) at different points in space. The situation studied here (breakdown) is far from equilibrium. The distribution in this case tends to drop more rapidly at high energy than at low energy, which means that as the particles go 'upstream' there will be a decrease in mean energy, even in the absence of collisions. We are effectively treating our distribution as being monoenergetic, with no tail; every particle in effect has the same energy, and if they go upstream their kinetic energy drops because their potential energy goes up. In reality, the distribution has a tail and some of the less energetic particles cannot move upstream while the more energetic particles can go upstream. In a Maxwellian, the particles which are found upstream have the same mean kinetic energy as the group they came from, despite individual particles losing kinetic energy, because they came from the tail with the correct energy distribution to maintain the mean kinetic energy as they move in a potential well. It would be possible to conserve energy and still allow the particles to have the mean energy as they go upstream. This would be done by subtracting enough energy from the cell they started in (cell i) to allow the particles which went upstream (to cell $i+1$) to have been the high-energy tail of the distribution. Let the mean energy in cell i be κ and the potential energy difference between cell $i+1$ and cell i be

$$W = -q(V[i+1] - V[i]).$$

Suppose the tail particles have a mean kinetic energy of $\kappa + W$ in cell i. Then the particles' final mean kinetic energy (in cell $i+1$) would be κ but their potential energy would be W per particle higher than in cell i. If n particles moved from i to $i+1$, then $n(\kappa + W)$ would be subtracted from the total energy in cell i. This is not justifiable here, however. Methods to make the fluid model more accurate will be discussed later.

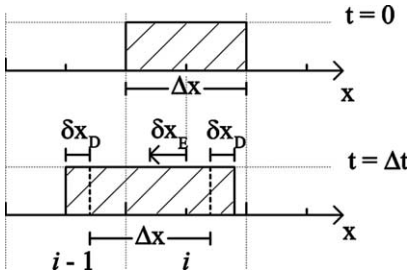

Fig. 3. A cell moves by $\delta x_E = -0.3\Delta x$ and gets expanded by $\delta x_D = 0.2\Delta x$ after a time-step Δt.

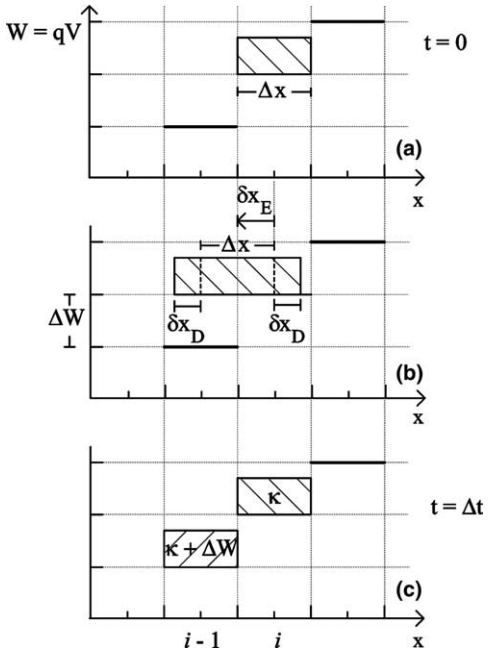

Fig. 4. The schematic shows how the moving cell in 'fluid – $R(\kappa)$' moves and conserves energy. (a) The particles in the initial cell have mean energy κ. (b) The fluid cell moves by a distance δx_E and expands in length by δx_D. (c) After a time step Δt, a fraction of particles in the original cell is put in the final cell with the mean energy of $\kappa + \Delta W$.

2.2.3. Propagator method and finite difference scheme

The proposed propagator method, applied to the case where δx_E and δx_D are both less than $0.5\Delta x$ (for both $\delta x_E > \delta x_D$ and $\delta x_E < \delta x_D$) can be seen to give reasonable finite difference (FD) expressions. To show this, we consider applying the propagator to a single initial cell. The propagator moves the initial cells one at a time and redistributes them – it does not consider final cells one at a time, as in FD. Consider $\delta x_E = 0$ and from Eq. (5), with Δt very small, $\Delta t < 2(\Delta x)^2/D$,

$$\delta x_D = D\frac{\Delta t}{\Delta x}. \tag{13}$$

Now consider the FD approach. For an initial density n_i in cell i, and with all other densities equal to zero, we will say that there is a flux

$$\Gamma_D = \frac{Dn_i}{\Delta x} \tag{14}$$

flowing into each neighbor cell. The number of particles entering the cell in Δt is $\Gamma_{\mathrm{D}}\Delta t$; the change of density in the neighbor cell is

$$\Delta n = \frac{D\Delta t}{(\Delta x)^2} n_i. \tag{15}$$

This is equivalent to the usual FD expression. It is also equivalent to our propagator, where we say that the initial cell expanded by a length δx_{D}. The overlap rule will place a fraction f of the contents in cell i into cell $i + 1$, where

$$f = \frac{\delta x_{\mathrm{D}}}{\Delta x + 2\delta x_{\mathrm{D}}}. \tag{16}$$

Then for $\delta x_{\mathrm{D}} \ll \Delta x$,

$$f = \frac{D\Delta t}{(\Delta x)^2} \tag{17}$$

in agreement with above. Similar arguments can be made in regard to the drift term. Similarly, the energy conserving aspect of the propagator can also be reduced to the FD expression, when $\delta x_{\mathrm{E}},\ \delta x_{\mathrm{D}} \ll \Delta x$, and $\delta x_{\mathrm{D}} < \delta x_{\mathrm{E}}$. Suppose that the particle density in an initial cell i is n_i. The change in energy of the cell i due to cell $i + 1$, according to our energy conserving propagator, is

$$\Delta(n\bar{\mathscr{E}})_i = \frac{n_{i+1}\bar{\mathscr{E}}_{i+1}\delta x_{i+1}}{\Delta x} \tag{18}$$

$$= \frac{n_{i+1}\bar{\mathscr{E}}_{i+1}\boldsymbol{v}_{\mathrm{d}r}}{\Delta x}(\Delta t), \tag{19}$$

where $\delta x_{i+1} = \boldsymbol{v}_{\mathrm{d}r}\Delta t$, and $\boldsymbol{v}_{\mathrm{d}r}$ is a drift velocity which denotes the net effect of mobility and diffusion. The change in energy in the cell i due to losses of particles from cell i and due to heating in Δt is

$$\Delta(n\bar{\mathscr{E}})_i = Q_i\Delta t - \frac{n_i\bar{\mathscr{E}}_i\delta x_i}{\Delta x}, \tag{20}$$

where Q_i is the heating rate. Combined, these are equivalent to an upwind FD version of the equation of conservation of energy,

$$\frac{\partial(n\bar{\mathscr{E}})}{\partial t} + \frac{\partial(n\bar{\mathscr{E}}\boldsymbol{v}_{\mathrm{d}r})}{\partial x} = Q_i. \tag{21}$$

2.2.4. Fitting fluid parameters from the kinetic model

To derive a fluid model which matches the kinetic simulation as closely as possible, we generate the steady state electron distribution f_{e}, in a homogeneous plasma for a given electric field. We then load this distribution into a single cell i of the spatial mesh, and calculate the fractions of the particles in cell i moving into neighboring cells in N time steps of length Δt. We calculate effective values of the diffusion coefficient, D_{eff} and mobility, μ_{eff} that reproduce the mean position and the width of the curve. (The use of a single cell is consistent with the principle of superposition which underlies the propagator method. The result for any spatial profile can be constructed by use of a sum of densities in single cells, so no generality is lost in this way. Deformations in phase space are properly taken into account in the CS. In the limit of using many cells, the procedure follows particles along their orbits throughout the entire phase space – equivalent to using a particle simulation to follow their orbits, but putting particles back into phase space

cells occasionally. This procedure describes the deformation in the shape in phase space, although this may not be evident if one only considers the fate of one cell. Considering one cell is somewhat like considering one particle in a particle simulation, which might not show how the phase space volume evolves. The propagator used in calculation of the distribution function tracks the motion of the particles in phase space very accurately, employing the relevant conservation laws explicitly. The only errors expected from it are a modest amount of numerical diffusion caused by the finite mesh size. The method has been used in the past and calibrated carefully in a wide range of settings which lend support to these claims (see e.g. [9,10,42,43])). The values of $D_{\rm eff}$ and $\mu_{\rm eff}$ are obtained as functions of electric field, $\boldsymbol{E}$, and also the mean kinetic energy, κ, as are the ionization rate, I, and the fraction of the energy used in ionization, α. We then have the option of running the fluid code in a mode where all quantities ($D_{\rm eff}, \mu_{\rm eff}, I, \alpha$) are found from $\boldsymbol{E}$ which is denoted as 'fluid – $R(E)$'. Alternatively we can find the mean kinetic energy κ in each cell i by conserving energy and finding ($D_{\rm eff}, \mu_{\rm eff}, I, \alpha$) from κ, denoted as 'fluid – $R(\kappa)$'. (In general, in a time-dependent energy conserving code, κ is not simply a function of $\boldsymbol{E}$, so one does not expect that, e.g. $\mu \equiv \mu(\kappa)$ implies $\mu \equiv \mu(\boldsymbol{E})$.) The potential in the cells is treated as a staircase [10] and the change in kinetic energy is found as usual in the CS [10]. The energy conserving code is more accurate; exact energy conservation makes a noticeable difference.

2.2.5. Length and time scales

There are (at least) two natural length scales in this problem; the mean free path, and the length scale for energy gain,

$$L_\epsilon = \frac{\epsilon_c}{q \mid \boldsymbol{E} \mid}, \tag{22}$$

where $\epsilon_{\rm c}$ is some characteristic energy. $\epsilon_{\rm c}$ could be the mean particle energy, but for now let us suppose it is the ionization energy. To make our point better, let us further divide L_ϵ by α, so that L_{ϵ_i} becomes the distance we expect electrons to go before each electron causes an ionization. The density of electrons has the capability of rising exponentially, on the scale of L_{ϵ_i}. It is thus not reasonable to expect the density to be uniform on the scale of L_{ϵ_i}, and one should choose the mesh size

$$\Delta x \ll L_{\epsilon_i}. \tag{23}$$

However, the length scale of $L_\epsilon = \epsilon_{\rm c}/q|\boldsymbol{E}|$ is also an upper limit on the mesh size, if we are to be able to calculate the mean electron energy, and if α is small this scale is considerably smaller than L_{ϵ_i}. Similar remarks apply to the time step Δt. (There may be some variant of the Scharfetter–Gummel (SG) scheme [37] which could be derived to fit this situation. The SG scheme allows electron density in a semiconductor to be described semi-analytically, so that the exponential variation is captured on a mesh which would otherwise be much too small. The SG scheme is not directly applicable, however.)

The time scale $\tau_{\rm inel}$ for inelastic collisions of energetic particles is of the order of $10\tau_{\rm el}$. A large fraction (essentially all) of the particles have enough energy to undergo some sort of inelastic collision. It is important in any of these simulations to ensure that the fraction of the energy lost to inelastic processes at each time step is small, otherwise the energy will fluctuate unphysically. This means that even in a fluid model we should expect to take steps $\Delta t \ll \tau_{\rm inel}$. If the particles go a long way in space in going to the next spatial cell, they will artificially gain a great deal of energy and will do considerably more ionization than they should, because they will reach an energy where ionization is likely, without having to pass through lower energies where excitation dominates. A large Δx is thus particularly problematic, and it is compounded since the density is growing exponentially so small errors rapidly become large ones. This artifact would appear to only exist in an energy-conserving scheme, but the problem with large Δx is not removed in the scheme which does not conserve energy (see the next section). In the next section the results of the full CS and 'Fluid' models will be shown and compared.

3. Simulation results

3.1. Mesh size and time step in the propagator method – fluid model

This section considers the effect of increasing Δx and Δt in the fluid model. While our study is for the propagator method we expect our main conclusions to hold for an energy-conserving FD scheme.

Both of the fluid simulations, fluid – $R(\kappa)$ and fluid – $R(E)$ (where $R(\kappa)$ denotes a fluid code using $(D_{\text{eff}}, \mu_{\text{eff}}, I, \alpha)$ as functions of mean kinetic energy κ, and $R(E)$ denotes a fluid code using $(D_{\text{eff}}, \mu_{\text{eff}}, I, \alpha)$ as functions of electric field E) have been scrutinized, on a mesh on which the kinetic simulation is converged ($\Delta x = 2.5 \times 10^{-7}$ m and $\Delta t = 5.0 \times 10^{-14}$ sec serves as a base case), as well as on the mesh with ten times the mesh spacing ($10\Delta x$), and with time step ($\Delta t, 10\Delta t, 20\Delta t, \ldots, 100\Delta t$). The fluid models are employed to simulate a dielectric barrier discharge in N_2 (0.3 mm gap between two 0.9 mm dielectric slabs ($\epsilon_r \sim 3.0$)) at atmospheric pressure. The $R(E)$ model, on the base mesh $(\Delta x, \Delta t)$, gives considerably higher densities than the kinetic model. The $R(\kappa)$ model does well in the comparison to the kinetic model, which will be discussed in the next section. We thus focus on the $R(\kappa)$ model, since the $R(E)$ model is not reliable even on the base mesh [32–36].

Comparing the energy conserving – $R(\kappa)$ simulations, without ionization, the peak positions of the densities for all cases are in the same place at the same time, with approximately 10% variation in magnitude as seen from Fig. 5(a). A slightly different diffusion coefficient D is evident. Corrections to the variance of the pulses can be calculated and applied to the propagator if needed but, unlike the correction to the mean displacement, it has not been done here. On the other hand, in the presence of ionization, the electrons tend to move faster (see Fig. 5(b)). The mean energy in the case with ionization is lower than in that without ionization and consequently a bigger value of μ is used; as a result, the electrons move faster (Fig. 6). With ionization, for a mesh spacing of $10\Delta x$ with Δt, and $10\Delta t$, the electrons start to go faster. The density also rises faster with time as Δt is increased, and in fact the density starts to grow unphysically large (the run goes unstable for $t \gtrsim 20\Delta t$). This is despite the fact that the time step is well below the Courant limits and the dielectric relaxation time.

The fluid – $R(E)$ scheme does not go unstable and is reproducible up to quite large values of Δt. The behavior of the $R(E)$ method is not surprising – the problem with large Δx and Δt is caused by energy conservation. Fig. 7 shows the electron densities resulting from the fluid – $R(E)$ simulations without and with ionization. The $R(E)$ scheme with the bigger mesh size $(10\Delta x, \Delta t)$ and $(10\Delta x, 10\Delta t)$, gives lower electron density than the base case $(\Delta x, \Delta t)$ by about 10%. The $(10\Delta x, 100\Delta t)$ case brings the density back closer to the base case, especially in the absence of ionization.

To show the effects of the use of wide range of Δx and Δt, the fluid – $R(\kappa)$ model is used to simulate a 5 mm discharge of Nitrogen gas between two 1.5 cm dielectric slabs. The electron densities at 1, 1.5, and 2 ns without and with ionization are shown in Fig. 8(a) and (b) consecutively. We observe (a) that in the absence of ionization, the results are virtually indistinguishable. This demonstrates that the propagator works as intended, for all Δx and Δt considered. However, (b) when ionization is added, the agreement is lost. As we argue throughout this paper, only the smallest Δx and Δt are suitable for studying the discharge during breakdown. This is not a limitation of the propagator, which does not handle ionization. This limit is imposed by the need to use small Δx to resolve energy balance in the presence of ionization and in a very strong electric field.

In conclusion, an energy conserving scheme is needed for accuracy, but energy conservation limits us to $\Delta x \lesssim \lambda/2$ and $\Delta t \ll \tau_c$. The real limit on Δx in the fluid simulations may be that $\Delta x \ll L_{e_i}$ (say $\Delta x \sim 10\% L_e$); this limit is likely to be important in the kinetic simulations as well. (We emphasize that these limits are not only for this method; they are for any simulation of breakdown that operates at the level of the kinetic or fluid equations.)

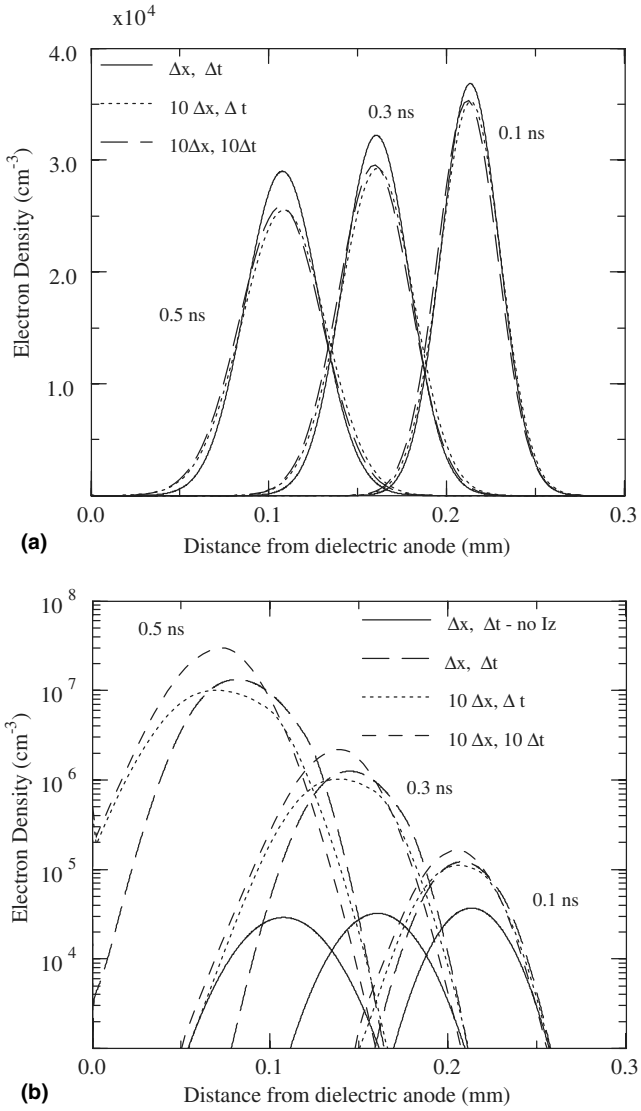

Fig. 5. Time evolution of electron densities calculated from the fluid – $R(\kappa)$. (a) Without ionization. (b) With ionization, comparing to the base case $(\Delta x, \Delta t)$ and without ionization (solid line).

There is a considerable literature, for instance, [22–30] on the use of flux-corrected transport (FCT) to correct for numerical diffusion (ND). ND, in the sense the term is usually used, does not appear to be the main problem in this work. Using different values of $(\Delta x, \Delta t)$ in Fig. 8(a) (see later in Section 3.2) made essentially no difference, which shows that ND is not an issue in those runs. Further, in Fig. 8(b) and other runs reported here, the case with $(10\Delta x, 10\Delta t)$ gives less good results than our base case, whereas if the usual ND were the problem, the $(10\Delta x, 10\Delta t)$ case would perform better. For these reasons, and in the light of the discussion in Section 2.2.5, we do not expect FCT to remedy the problem with energy conservation which occurs when Δx is large.

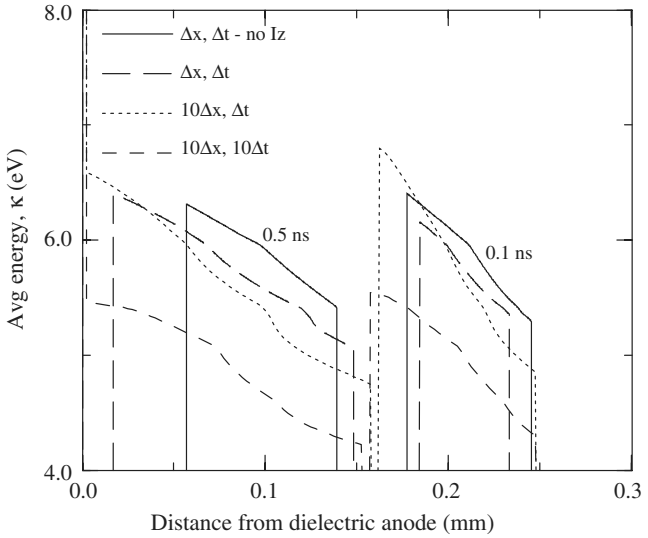

Fig. 6. Time evolution of average kinetic energy of electrons, compared to the base case – $(\Delta x, \Delta t)$ and without ionization (solid line) calculated from the fluid – $R(\kappa)$.

3.2. Comparison of numerical models

Here, we have employed the full kinetic model, the fluid – $R(\kappa)$ model, and the fluid – $R(E)$ model to simulate a similar discharge geometry as in the previous section. Since the kinetic CS requires a long run-time and large computer usage, a shorter discharge, with a 0.2 mm gap between two 0.6 mm dielectric slabs, is simulated.

A series of simulations has been done which illustrate the behavior of the models. These were initialized with a very small number of electrons so that the electric field in the discharge is constant at first ($|\boldsymbol{E}| = 6.66 \times 10^4$ V/cm). The time evolution of the number of electrons calculated from the models is shown in Fig. 9.

The density plots show that the fluid – $R(\kappa)$ model agrees very well with the full CS. The fluid – $R(E)$, on the other hand, overestimates the density by an exponentially growing factor. It overestimates most noticeably on the upstream side, because without energy conservation, it allows electrons which should have very little energy to diffuse upstream (to a higher potential energy region) and do ionization; hence the number of electrons is overestimated.

3.3. Simulations in AC field

To show the effectiveness and validate the accuracy of the proposed fluid model, in this section, the kinetic model (CS) and the fluid – $R(\kappa)$ model were employed in an AC electric field. The geometry is as for the DC field, (0.2 mm Nitrogen DBD at atmospheric pressure) supplied by a 4 kV source with frequency of 300.0 GHz, the highest frequency for which the transport coefficients (the mobility and diffusion coefficient) and the parameter α are valid, since they have all been obtained in the collisional limit. The growth rates of the electron density, for various amplitudes of the electric field within the same range as the DC field, have been obtained and illustrated in Fig. 10. The CS results are consistently slightly below the fluid results, because the CS runs are converging rather slowly to essentially the same value as the fluid. The growth rates for the AC field are lower than those for the DC field. This is probably because the AC discharge has a

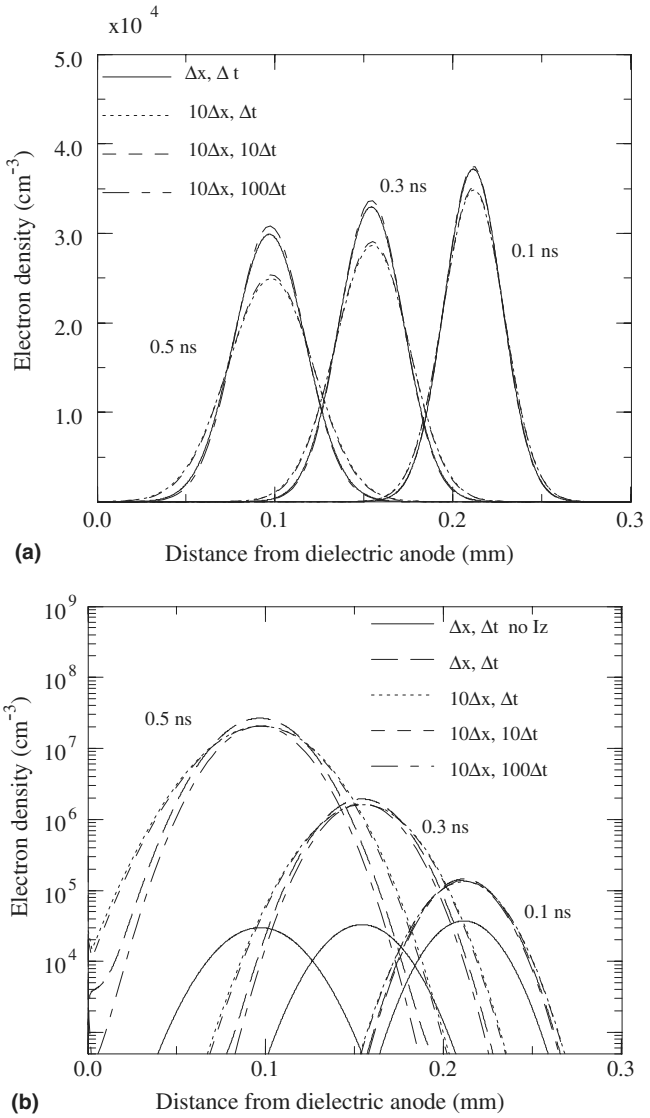

Fig. 7. Time evolution of electron densities calculated from the fluid – $R(E)$. (a) Without ionization. (b) With ionization compared to the base case $(\Delta x, \Delta t)$ and without ionization (solid line).

lower average field, thus the electrons gain a lower mean kinetic energy, and both the power and α are consequently lower.

4. Conclusions

In summary, we have developed and employed a propagator method within fluid models of gas breakdown; $R(\kappa)$ and $R(E)$, as well as a kinetic CS model. The $R(\kappa)$ and kinetic CS models can be made to agree

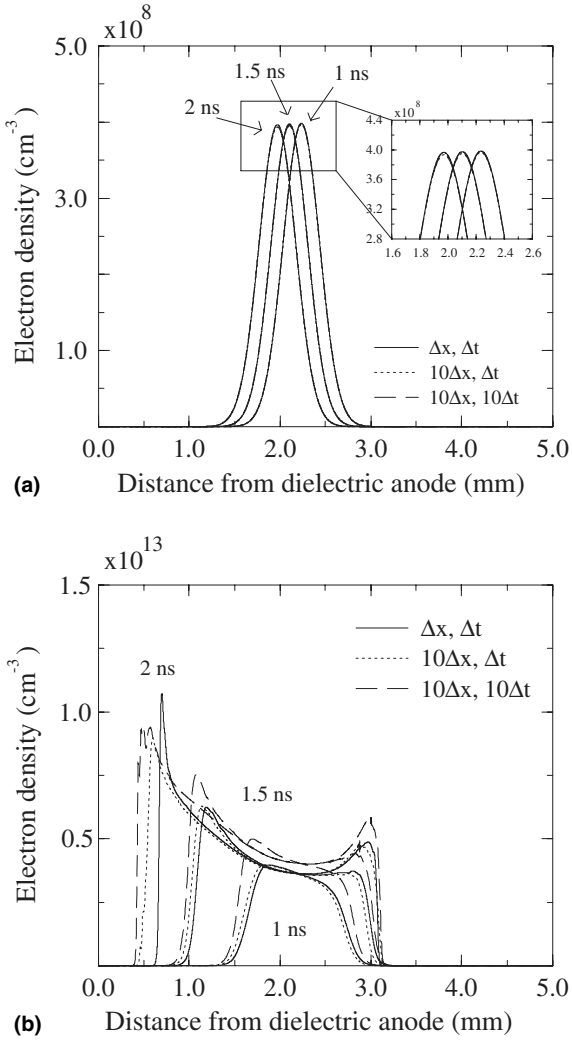

Fig. 8. Electron densities calculated from the fluid – $R(\kappa)$. (a) Without ionization. (b) With ionization, compared to the base case $(\Delta x, \Delta t)$ at time 1, 1.5, and 2 ns.

well subject to certain restrictions. The restrictions are first, that, in the kinetic code, rather fine resolution is needed.

Within fluid codes, a code employing energy conservation ($R(\kappa)$) is distinctly preferable. Perhaps surprisingly, the fluid code – $R(\kappa)$ must employ similarly small Δx (and Δt) as the kinetic code. Within the propagator method, it was necessary to calculate a set of corrections for the displacement δx_{E} which ensure that $\delta\bar{x} = \delta x_{\mathrm{E}}$. Consequently, the propagator method gives very close agreement in predicted densities (in the absence of ionization) over a wide range of Δx and Δt. The fluid model using propagator method and the kinetic model (CS) have also been briefly studied with an AC field.

One of the issues which we plan to investigate in future is the possibility of allowing for the particles leaving a cell being more or less energetic than the average. We will attempt to tabulate the energy that particles have, when traveling up and downstream, as a function of the mean energy in the initial cell

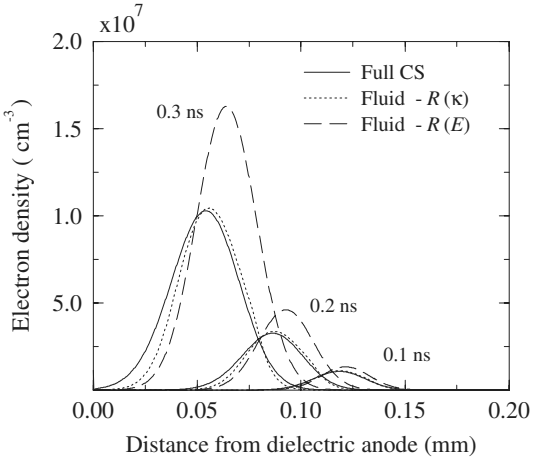

Fig. 9. Time evolution of electron densities calculated from kinetic CS, and fluid – $R(\kappa)$, and $R(E)$ models.

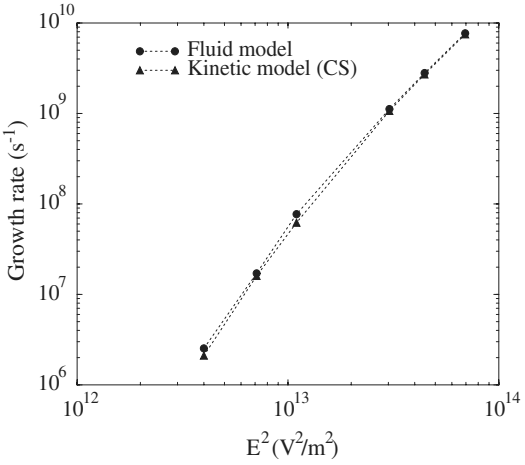

Fig. 10. Growth rates of electron density as a function of electric field squared (E^2).

and of the electric field. Then we will be able to allow particles leaving a cell to have more energy than the mean energy in that cell. That energy will be subtracted from the total in the initial cell, to maintain energy conservation. We will also calculate a separate value for α for the injected particles newly entering a cell, since α will be a different function of kinetic energy for injected particles than it is for the particles which stay in a cell.

Acknowledgment

We acknowledge the suggestions of V.I. Kolobov and M.J. Kushner (especially for the cross-section data [49]).

Appendix A. The list of mean displacement corrections for δx_E

See Table A.1.

Table A.1
The corrections of mean displacement, $\delta x'_E$, for δx_E

Condition			Value of $\delta x'_E$
(A) $\lvert\delta x_E\rvert < \delta x_D$			
$\lvert\delta x_E\rvert + \delta x_D \leqslant \Delta x$			$\frac{-\lvert\delta x_E\rvert}{2\Delta x} C_l$ [*]; but if $\lvert\delta x'_E\rvert > \delta x_D$ [a], $\delta x'_E = -\left[\frac{\lvert\delta x_E\rvert}{\Delta x} C_l - \delta x_D\right]$
$\lvert\delta x_E\rvert + \delta x_D \geqslant \Delta x$	If $\lvert\delta x_E\rvert \& \delta x_D \geqslant \Delta x$		δx_E
	else		$-\frac{1}{3}\left[\frac{\lvert\delta x_E\rvert}{\Delta x} C_l - \delta x_D + \Delta x\right]$
(B) $\lvert\delta x_E\rvert > \delta x_D$			
$\lvert\delta x_E\rvert + \delta x_D \leqslant \Delta x$			$-\left[\frac{\lvert\delta x_E\rvert}{\Delta x} C_l - \delta x_D\right]$; but if $\lvert\delta x'_E\rvert < \delta x_D$ [a] $\delta x'_E = -\frac{\lvert\delta x_{rmE}\rvert}{2\Delta x} C_l$
$\lvert\delta x_E\rvert + \delta x_D \geqslant \Delta x$	If $\lvert\delta x_E\rvert \& \delta x_D \geqslant \Delta x$		δx_E
	If $\lvert\delta x_E\rvert \leqslant \Delta x$		$-\frac{1}{2}\left[\frac{\lvert\delta x_E\rvert}{\Delta x} C_l - 2\delta x_D + \Delta x\right]$
	If $\lvert\delta x_E\rvert \geqslant \Delta x$, $\lvert\delta x_E\rvert + \delta x_D \leqslant 2\Delta x$	$\delta x_D \leqslant \delta x_E - \underline{\text{int}}(\delta x_E)$	$-\left[\frac{\lvert\delta x_E\rvert}{\Delta x} C_l - 3\delta x_D\right]$
		else	$-\frac{1}{2}\left[\frac{\lvert\delta x_E\rvert}{\Delta x} C_l - 2\delta x_D + \Delta x\right]$
	else		δx_E

[a] This condition must be checked after the correction since it might change the case from A to B and vice versa.
[*] $C_l = \Delta x + 2\delta x_D$.

References

[1] N.L. Aleksandrov, I.V. Kochetov, Electron rate coefficients in gases under non-uniform field and electron density conditions, J. Phys. D 29 (1996) 1476.
[2] J.P. Verboncoeur, G.J. Parker, B.M. Penetrante, Comparison of collision rates in particle-in-cell, monte carlo, and Boltzmann codes, J. Appl. Phys. 80 (1996) 1299.
[3] M.J. Kushner, Monte-Carlo simulation of electron properties in RF parallel plate capacitively coupled discharges, J. Appl. Phys. 54 (1983) 4958.
[4] M.J. Kushner, Mechanisms for power deposition in Ar/SiH_4 capacitively coupled RF discharges, IEEE Trans. Plasma Sci. 14 (1985) 188.
[5] R.T. Farouki, S. Hamaguchi, M. Dalvie, Monte carlo simulations of space-charge-limited ion transport through collisional plasma sheaths, Phys. Rev. A 44 (1991) 2264.
[6] M. Surendra, D.B. Graves, Particle simulations of radio-frequency glow discharges, IEEE Trans. Plasma Sci. 19 (1991) 144.
[7] W.J. Goedheer, P.M. Meijer, Kinetic modeling of positive ions in a low-pressure RF discharge, IEEE Trans. Plasma Sci. 19 (1991) 245.
[8] M.J. Brennan, Optimization of monte carlo codes using null collision techniques for experimental simulation at low E/N, IEEE Trans. Plasma Sci. 19 (1991) 256.
[9] W.N.G. Hitchon, Plasma Processes for Semiconductor Fabrication, Cambridge University Press, Cambridge, MA, 1999.
[10] J. Feng, W.N.G. Hitchon, Self-consistent kinetic simulation of plasmas, Phys. Rev. E 61 (2000) 3160.
[11] W.N.G. Hitchon, D.J. Koch, J.B. Adams, An efficient scheme for convection-dominated transport, J. Comput. Phys. 83 (1989) 79.
[12] A.J. Christlieb, W.N.G. Hitchon, E.R. Keiter, A computational investigation of the effects of varying discharge geometry for an inductively coupled plasma, IEEE Trans. Plasma Sci. 28 (2000) 2214.
[13] Y. Matsunaga, T. Hatori, T. Kato, Kinetic simulation of nonlinear phenomena of an ion acoustic wave in gas discharge plasma with convective scheme, Phys. Plasma 8 (2001) 1057.
[14] Y. Matsunaga, T. Hatori, T. Kato, Kinetic simulation of an ion acoustic wave with charge exchange process in direct current discharge plasma, J. Phys. Soc. JPN 71 (2002) 2445.
[15] J. Bretagne, G. Gousset, T. Simko, Ion-transport simulation in a low-pressure hydrogen gas at high electric-fields by a convective-scheme method, J. Phys. D 27 (1994) 1866.

[16] V.P. Konovalov, J. Bretagne, G. Gousset, On the distribution of positive-ions in the cathode region of a gas-discharge, J. Phys. D 25 (1992) 1073.
[17] P. Bayle, J. Vaquie, M. Bayle, Cathode region of a transitory discharge in CO_2. I. theory of the cathode region, Phys. Rev. A 34 (1986) 360.
[18] Y.H. Oh, N.H. Choi, D.I. Choi, A numerical simulation of RF glow discharge containing an electronegative gas composition, J. Appl. Phys. 67 (1990) 3264.
[19] J.P. Boeuf, A two-dimensional model of DC glow discharge, J. Appl. Phys. 63 (1988) 1342.
[20] J.D.P. Passchier, W.J. Goedheer, A two-dimensional fluid model for an argon RF discharge, J. Appl. Phys. 74 (1993) 3744.
[21] M.S. Barnes, T.J. Cotler, M.E. Elta, Large-signal time-domain modeling of low-pressure RF glow discharges, J. Appl. Phys. 61 (1987) 81.
[22] J. Li, S.K. Dhali, Simulation of microdischarges in a dielectric-barrier discharge, J. Appl. Phys. 82 (1997) 4205.
[23] N.L. Aleksandrov, E.M. Bazelyan, V.A. Vasil'ev, The effect of low direct voltage on streamer breakdown in long non-uniform air gaps, J. Phys. D 36 (2003) 2089.
[24] G. Steinle, D. Neundorf, W. Hiller, M. Pietralla, Two-dimensional simulation of filaments in barrier discharges, J. Phys. D 32 (1999) 1350.
[25] N.L. Aleksandrov, E.M. Bazelyan, Simulation of long-streamer propagation in air at atmospheric pressure, J. Phys. D 29 (1996) 740.
[26] W.G. Min, H.S. Kim, S.H. Lee, W.Y. Hahn, An investigation of FEM-FCT method for streamer corona simulation, IEEE Trans. Magn. 36 (2000) 1280.
[27] W.G. Min, H.S. Kim, S.H. Lee, W.Y. Hahn, A study on the streamer simulation using adaptive mesh generation and FEM-FCT, IEEE Trans. Magn. 37 (2001) 3141.
[28] J.M. Guo, C.J. Wu, Comparison of multidimensional non-equilibrium and equilibrium fluid and monte carlo models for streamers, J. Phys. D 26 (1993) 487.
[29] J.M. Guo, C.J. Wu, Two-dimensional nonequilibrium fluid models for streamers, IEEE. Trans. Plasma Sci. 21 (1993) 684.
[30] E.E. Kunhardt, C. Wu, Toward a more accurate flux corrected transport algorithm, J. Comput. Phys. 68 (1987) 127.
[31] M.S. Barnes, T.J. Cotler, M.E. Elta, A staggered-mesh finite-difference numerical-method for solving the transport-equations in low-pressure RF glow-discharges, J. Comput. Phys. 77 (1988) 53.
[32] R.J. Carman, R.P. Mildren, Computer modelling of a short-pulse excited dielectric barrier discharge xenon excimer lamp ($\lambda \sim 172$ nm), J. Phys. D 36 (2003) 19.
[33] R.J. Carman, R.P. Mildren, Computer modeling of electrical breakdown in a pulsed dielectric barrier discharge in xenon, IEEE Trans. Plasma Sci. 30 (2002) 154.
[34] Z. Kanzari, M. Yousfi, A. Hamani, Modeling and basic data for streamer dynamics in N_2 and O_2 discharges, J. Appl. Phys. 84 (1998) 4161.
[35] A. Oda, Y. Sakai, H. Akashi, H. Sugawara, One-dimensional modelling of low-frequency and high-pressure Xe barrier discharges for the design of excimer lamps, J. Phys. D 32 (1999) 2726.
[36] A. Oda, H. Sugawara, Y. Sakai, H. Akashi, Estimation of the light output power and efficiency of Xe barrier discharge excimer lamps using a one-dimensional fluid model for various voltage waveforms, J. Phys. D 33 (2000) 1507.
[37] D.L. Scharfetter, H.K. Gummel, Large-signal analysis of a silicon read diode oscillator, IEEE T. Electron Dev. 16 (1969) 64.
[38] M.F. Wehner, W.G. Wolfer, Numerical evaluation of path-integral solutions to Fokker–Planck equations, Phys. Rev. E 27 (1983) 2663.
[39] James W. Eastwood, Particle simulation methods in plasma physics, Comput. Phys. Commun. 43 (1986) 89.
[40] James W. Eastwood, The stability and accuracy of EPIC algorithms, Comput. Phys. Commun. 44 (1987) 73.
[41] J.B. Adams, W.N.G. Hitchon, Solution of master and Fokker–Planck equations by propagator methods, Applied to Au/NaCl thin film nucleation, J. Comput. Phys. 76 (1988) 159.
[42] W.N.G. Hitchon, G.J. Parker, J.E. Lawler, Physical and numerical verification of discharge calculations, IEEE Trans. Plasma Sci. 21 (1993) 228.
[43] G.J. Parker, W.N.G. Hitchon, J.E. Lawler, Self-consistent kinetic model of an entire DC discharge, Phys. Lett. A 174 (1993) 308.
[44] A. Staniforth, J. Cote, Semi-Lagrangian integration schemes for atmospheric models, Monthly Weather Rev. 119 (1991) 2206.
[45] T.J. Sommerer, W.N.G. Hitchon, R.E.P. Harvey, J.E. Lawler, Self-consistent kinetic calculations of helium RF glow discharge, Phys. Rev. A 43 (1991) 4452.
[46] R.J. Purser, L.M. Leslie, An efficient semi-Lagrangian scheme using third-order semi-implicit time integration and forward trajectories, Monthly Weather Rev. 122 (1994) 745.

[47] L.M. Leslie, R.J. Purser, Three-dimensional mass-conserving semi-Lagrangian scheme employing forward trajectories, Monthly Weather Rev. 123 (1995) 2551.
[48] R.D. Nair, J.S. Scroggs, F.H.M. Semazzi, A forward-trajectory global semi-Lagrangian transport scheme, J. Comput. Phys. 190 (2003) 275.
[49] M.J. Kushner, Computational Optical and Discharge Physics Group, Dept. of Electrical and Computer Engineering, University of Illinois. Available from: <www.uigelz.ece.uiuc.edu/data.html>.